Contents lists available at ScienceDirect

Journal of Organometallic Chemistry

Mechanistic pathways for oxidative addition of aryl iodides to the low-ligated diethanolamine palladium(0) complex in phosphine-free Heck reactions

Zorica D. Petrović *, Vladimir P. Petrović, Dušica Simijonović, Svetlana Marković

Faculty of Science, University of Kragujevac, P.O. Box 60, 34000 Kragujevac, Serbia

ARTICLE INFO

ABSTRACT

A set of reactions of different activated olefins and aryl iodides with the *trans*-dichlorobis(diethanolamine-*N*)palladium(II) complex (*trans*-[PdCl$_2$(DEA)$_2$]) as a precatalyst was performed, in the presence of diethanolamine (DEA) as a weak base, and NaOEt as a strong base. It was established that the presence of NaOEt slightly lowered the yields, but significantly accelerated the reactions. This experimental finding is in agreement with our computational investigation that shows that significantly higher activation barrier is required for the preactivation reaction in the presence of a weak base than in the presence of a strong base. The reaction between the catalytically active DEA–Pd(0)–Cl complex, formed in the preactivation reaction, and iodobenzene was investigated using density functional theory. Two mechanisms for the oxidative addition of the activated complex were found. The first mechanism is based on a nucleophilic attack of Pd on I of iodobenzene, and yields an intermediate tetracoordinated Pd complex (aI2). The second mechanism begins with a nucleophilic attack of Pd on the benzene ring, and yields a tricoordinated intermediate complex (bI4). It was concluded, on the basis of structural and energetical properties of aI2 and bI4, that the second mechanism is significantly more favorable. It was shown that the oxidative addition requires noticeable lower activation energy than that required for the preactivation process. Thus, our investigations indicate that oxidative addition is not the rate determining step for the Heck reactions investigated in this work, but preactivation step.

1. Introduction

Organic reactions catalyzed with transition metals usually occur in series of steps. In each step, there are reactive intermediates as products, of which at least one contains σ carbon–metal bond. A class of such reactions includes palladium-catalyzed cross-coupling reactions of arylation of olefins, known as the Heck reactions [1–7]. These reactions have major impact on organic chemistry due to their significant synthetic versatility [8–10].

In our previous studies [11,12] we have elaborated the preactivation steps of a phosphine-free Heck reaction, where as a precatalyst we used *trans*-dichlorobis(diethanolamine-*N*)palladium(II) complex (*trans*-[PdCl$_2$(DEA)$_2$]). Synthesis and structural characterization of this complex has been reported in Ref. [13]. It was established that DEA–Pd(0)–Cl was obtained in the preactivation process of the investigated reaction (step **a**, Scheme 1).

The next step in the Heck catalytic cycle is oxidative addition of aryl halide to Pd(0) species. This step has been the subject of much investigation [14–21], and is considered to be the rate determining

process. Oxidtive addition usually involves coordinatively unsaturated Pd(0) complexes [15–17,21–23]. A lot of work has been devoted to the elucidation of the catalytic pathways where phosphines are used as ligands [14–18,22–24], whereas the results regarding non-phosphine ligands are scarced [19,20,25–31]. Hence, the aim of this experimental and DFT study is to investigate possible ways of oxidative addition of aryliodides to the preactivated Pd(0) complex (DEA–Pd(0)–Cl).

2. Results and discussion

Our recent experimental works confirmed that the *trans*-dichlorobis(diethanolamine-N)palladium(II) complex can be useful precatalyst in phosphine-free Heck reactions [11]. The mechanism of the initial preactivation process, solvent effects, and acceleration of the reaction induced with a strong base (NaOEt), were examined using density functional theory (DFT) [12]. It was deduced that the DEA–Pd(0)–Cl complex is obtained in step **a** of the reaction, and that it is catalytically active form (Scheme 1).

Now we investigate possible mechanistic pathways for oxidative addition, (step **b** in Scheme 1), of aryl iodides to the low-ligated diethanolamine palladium(0) complex. It is believed that oxidative addition is crucial and rate determining step of the Heck

* Corresponding author.
   E-mail address: zorica@kg.ac.rs (Z.D. Petrović).
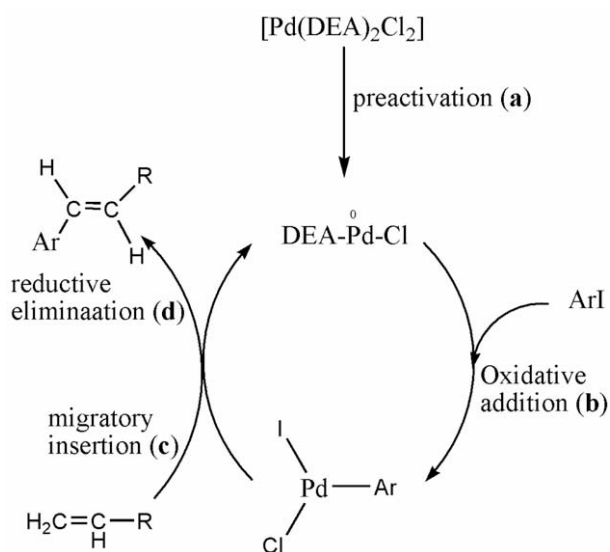
Scheme 1. Proposed mechanism for the catalytic cycle of the Heck reactions where *trans*-[PdCl$_2$(DEA)$_2$] is used as a precatalyst.

reactions, and therefore, very interesting for detailed research. Thus, we continued our assay of the Heck reactions, by performing a set of reactions of different activated olefines and aryl iodides with *trans*-[PdCl$_2$(DEA)$_2$] as a precatalyst, in the presence of DEA as a weak base, and in the presence of NaOEt as a strong base. The results of our experiments are presented in Table 1.

When the reactions were performed in the presence of DEA, 2 mol% of the *trans*-[PdCl$_2$(DEA)$_2$] complex was used at 110 °C. Reaction time of 12 h for iodobenzene, and 14 h for iodoanisole, was necessary to achieve good reaction yields. In order to increase the reaction rate, NaOEt was used instead of DEA. It was established that the use of 2 mol% of *trans*-[PdCl$_2$(DEA)$_2$] and NaOEt, significantly decreases the reaction time, from 12 to 8 h for iodobenzene, and from 14 to 10 h for iodoanisole, and that the desired coupling products **1–8** were obtained in good yields (Table 1). Moreover, when the reactions were perfermormed in the presence of DEA, as weak base, coordinating ligand and solvent, the yields of the reaction products were higher and catalyst precursor could be recovered and recycled. The precatalyst *trans*-[PdCl$_2$(DEA)$_2$] was recycled two times without significant loss in activity (the yields

of coupling products were to 5% lower). Table 1 shows that the yields of the coupling products are slightly lower for the reactions performed with NaOEt. When iodoanisole was used as electron-rich, and therefore less reactive aryl iodide, a certain amount of unreacted substrate remained in the reaction mixture, that directly results in lower product yields. In the case of the reactions where DEA was used as base and solvent, polymerization reaction was observed as competitive reaction (the polymerizations of acrylates by neutral palladium complexes are known in literature [31–33]). The competitive polimerization reaction, as well as electron-withdrawing and electron-donating substituent effects of different aryl iodides will be further examined.

Considerable stability of *trans*-[PdCl$_2$(DEA)$_2$] towards air and moisture, and simplicity of reaction procedure make investigated reactions atractive way of formation of new C–C bond between aromatic ring and activated olefins. Our experimental finding, that these versatile reactions occur faster in the presence of a strong base, is in agreement with our computational investigation that shows that significantly higher activation barrier is required for the preactivation reaction in the presence of a weak base (111.8 kJ/mol [12]) than in the presence of a strong base (83.0 kJ/mol [11]). We assume, on the basis of these facts, that the preactivation process is the rate determining step for the Heck reactions investigated in our laboratories. The purpose of our further computational research is to find out the activation energy for the oxidative addition, and compare it to those required for the preactivation reaction.

2.1. DFT study of the oxidative addition of iodobenzene to the DEA–Pd(0)–Cl complex

The reaction between the activated complex and iodobenzene was investigated using a DFT method. Two mechanisms for the oxidative addition of the activated complex were found. The general outline of these mechanisms is presented in Scheme 2. The first mechanism begins with a nucleophilic attack of palladium on iodine, thus forming the intermediate tetracoordinated complex (aI2 in Scheme 2) via intermediate aI1 and transition state aTS1 (pathway A). The second mechanism begins with an attack of palladium on benzene ring, and proceeds via transition states bTS1, bTS2, bTS3, and bTS4, and intermediates bI1, bI2, and bI3 (pathway B). The tricoordinated intermediate complex (bI4) is here yielded.

The optimized geometries of all transition states are presented in Fig. 2. The selected bond distances and bond angles of transition

Table 1
Reactions between activated olefins and aryl iodides catalyzed by *trans*-[PdCl$_2$(DEA)$_2$].

Entry	ArI	R	Base	Time (h)	Product number	Yield (%)[c]
1	C$_6$H$_5$I	C$_6$H$_5$	DEA[a]	12	**1**	87
2	C$_6$H$_5$I	C$_6$H$_5$	NaOEt[b]	8		82
3	C$_6$H$_5$I	COOCH$_3$	DEA	12	**2**	88
4	C$_6$H$_5$I	COOCH$_3$	NaOEt	8		80
5	C$_6$H$_5$I	COOC$_2$H$_5$	DEA	12	**3**	87
6	C$_6$H$_5$I	COOC$_2$H$_5$	NaOEt	8		83
7	C$_6$H$_5$I	COOC$_3$H$_7$	DEA	12	**4**	86
8	C$_6$H$_5$I	COOC$_3$H$_7$	NaOEt	8		82
9	C$_6$H$_5$I	COOC$_4$H$_9$	DEA	12	**5**	90
10	C$_6$H$_5$I	COOC$_4$H$_9$	NaOEt	8		87
11	C$_6$H$_5$I	COOC$_5$H$_{11}$	DEA	12	**6**	86
12	C$_6$H$_5$I	COOC$_5$H$_{11}$	NaOEt	8		82
13	CH$_3$OC$_6$H$_4$I	COOCH$_3$	DEA	14	**7**	76
14	CH$_3$OC$_6$H$_4$I	COOCH$_3$	NaOEt	10		74
15	CH$_3$OC$_6$H$_4$I	COOC$_4$H$_9$	DEA	14	**8**	74
16	CH$_3$OC$_6$H$_4$I	COOC$_4$H$_9$	NaOEt	10		72

[a] DEA (1 mmol) at 110 °C.
[b] NaOEt (0.2 mmol) at 90 °C.
[c] Isolated yield; only the *trans* product was detected by ^{1}H NMR.
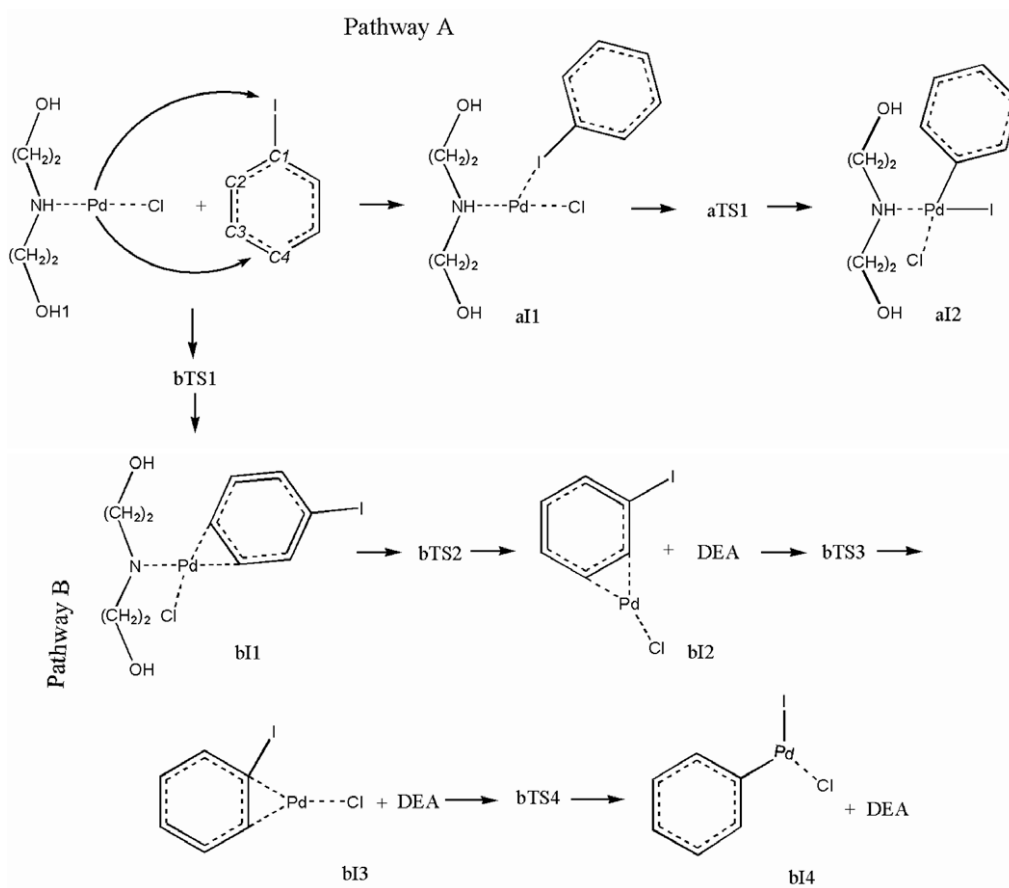
Scheme 2. Proposed mechanisms for oxidative addition of iodobenzene to the DEA–Pd(0)–Cl complex. aI1, aI2, bI1, bI2, bI3 and bI4 stand for intermediates, whereas aTS1, bTS2, bTS3, and bTS4 denote transition states in pathways A and B. DEA in Pathway B denotes the released molecule of solvent.
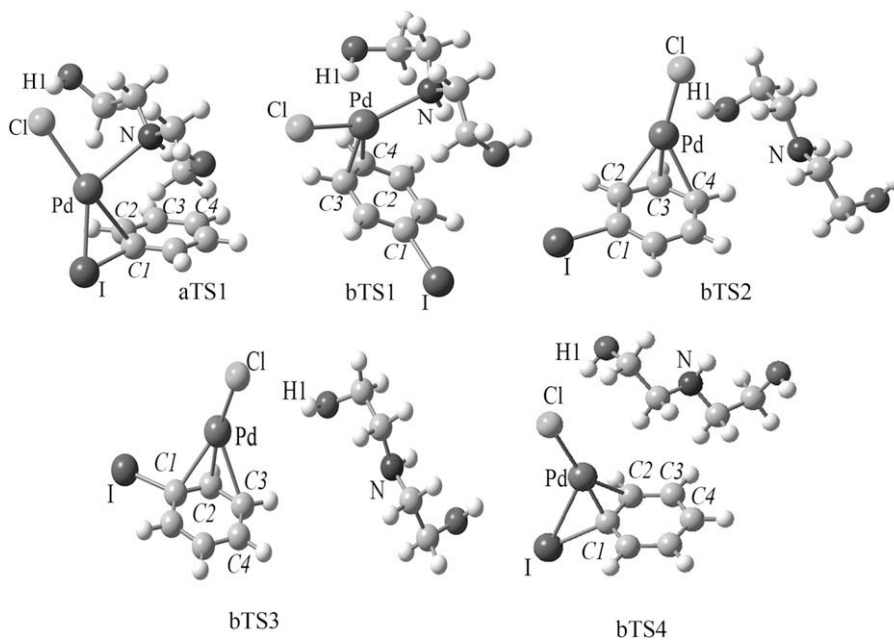
Fig. 1. Optimized geometries of transition states in the investigated reaction. See Scheme 1 for definition of symbols.

states and intermediates are given in Tables 2 and 3. The energetic diagram of the transformations is depicted in Fig. 1, whereas total energies, enthalpies, and free energies of all relevant species are provided in Table 1 of Supplementary material.

2.1.1. Pathway A

Fig. 3 shows the HOMO map of the activated complex and LUMO map of iodobenzene. The HOMO map delineates the area in the activated complex that is most electron-sufficient (Pd),

Fig. 2. Energetic diagrams for pathways A and B. R denotes the sum of free energies for the DEA–Pd(0)–Cl complex and iodobenzene.

Table 2
Selected bond distances for intermediates and transition states in pathways A and B. See Scheme 1 for definition of symbols.

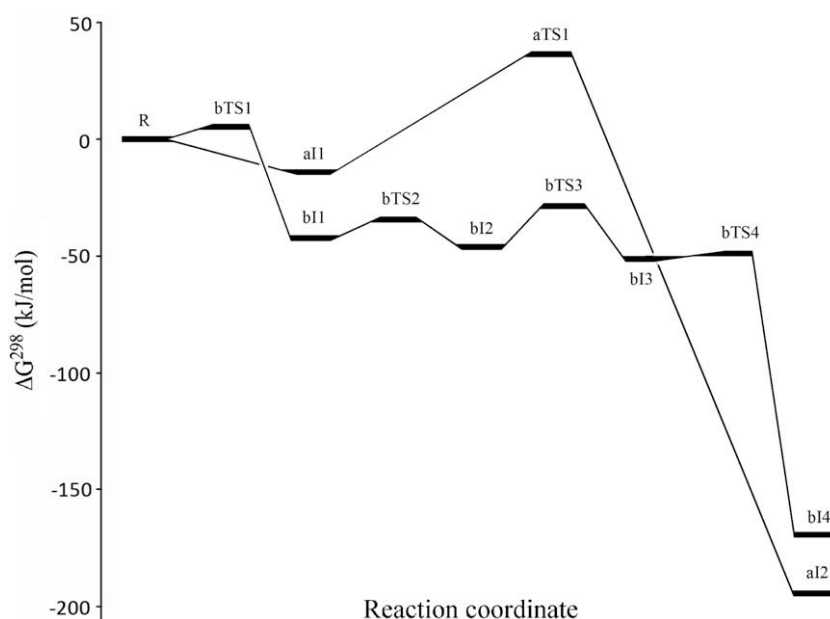|	Pd–N	Pd–I	Pd–Cl	Pd–C1	Pd–C2	Pd–C3	Pd–C4	Cl–H1	I–C1
aI1	2.21	2.92	2.38	–	–	–	–	–	2.26
aTS1	2.62	2.62	2.65	2.88	–	–	–	2.35	2.20
aI2	2.22	2.67	2.58	2.00	–	–	–	2.25	3.30
bts1	2.38	5.48	2.49	3.76	2.97	2.29	2.74	–	2.15
bi1	2.44	5.57	2.64	3.67	3.01	2.13	2.19	2.31	2.15
bts2	4.50	4.94	2.44	3.26	2.51	2.11	2.52	3.21	2.15
bi2	4.81	4.54	2.43	3.03	2.19	2.14	2.93	2.99	2.15
bts3	6.05	3.85	2.46	2.47	2.09	2.50	3.25	2.37	2.16
bi3	4.96	3.50	2.44	2.07	2.20	3.06	3.66	2.91	2.23
bts4	5.06	3.24	2.47	2.00	2.51	3.48	3.97	2.29	2.32
bi4	5.99	2.66	2.41	1.96	2.91	4.22	4.76	2.38	3.47

Table 3
Selected bond angles for intermediates and transition states in pathways A and B. See Scheme 1 for definition of symbols.

aI1	Cl–Pd–N 172.1	Cl–Pd–I 100.7	N–Pd–I 87.2	Pd–I–C1 173.8
aTS1	I–Pd–N 128.0	I–Pd–Cl 142.1	Cl–Pd–N 90.0	I–Pd–C1 46.8
aI2	I–Pd–N 178.5	C1–Pd–Cl 171.9	–	–
bTS1	N–Pd–Cl 146.5	C3–Pd–C4 31.1	C4–Pd–N 92.4	C3–Pd–Cl 95.2
bI1	N–Pd–Cl 93.8	C3–Pd–C4 39.0	C4–Pd–N 117.5	C3–Pd–Cl 108.6
bTS2	C3–Pd–Cl 163.3	C2–C3–Pd 88.1	C4–C3–Pd 88.7	–
bI2	C2–Pd–Cl 171.3	C3–Pd–Cl 149.2	C2–Pd–C3 38.6	–
bTS3	C2–Pd–Cl 163.4	C1–C2–Pd 87.3	C3–C2–Pd 88.3	–
bI3	C1–Pd–Cl 175.8	C2–Pd–Cl 145.3	C1–Pd–C2 38.9	–
bTS4	C1–Pd–Cl 176.0	I–C1–Pd 97.1		–
bI4	I–Pd–Cl 167.6	I–Pd–C1 96.1	Cl–Pd–C1 96.1	–

and agrees with the NBO analysis of the activated complex which shows that palladium bears five lone electron pairs in the d orbitals. On the other hand, the LUMO map delineates the area in iodobenzene that is most electron-deficient (I).

On the basis of these maps, one can expect that Pd of the activated complex will perform a nucleophilic attack on iodine of iodobenzene. Our calculations confirm this assumption. This step of the reaction proceeds smoothly, with the stabilization of the system (Table 1 in Supplementary material, and Fig. 1), and formation of aI1. As expected, the NBO charge on Pd of aI1 (-0.192) is increased in comparison to that in the activated complex (-0.361), whereas the NBO charge on I of aI1 (0.104) is decreased in comparison to that in iodobenzene (0.146). The NBO analysis of aI1 reveals five lone electron pairs in the d orbitals of Pd, where one of them shows a low occupancy of 1.72. This electron pair delocalizes into the σ bonding $0.76(sp^{3.65})_{C1} + 0.65(p)_I$ orbital. Pd is not involved in covalent bonding with the ligating atoms. Instead, there is a strong donation of density from the $sp^{2.96}$ orbital of Cl, $sp^{4.62}$ orbital of N, and almost pure s orbital of I to the formally empty $sd^{0.14}$ orbital of Pd. The HOMO and LUMO orbitals of aI1 are presented in Fig. 2. Both orbitals are delocalized, but the greatest contribution to the HOMO comes from Pd, and a significant contribution to the LUMO comes from the C1 atom. Thus, we examined a nucleophilic attack of Pd on C1 as the next step of pathway A. This step of the reaction occurs via transition state aTS1 (Fig. 2), requiring an activation barrier of 50.7 kJ/mol. The results of the intrinsic reaction coordinate (IRC) calculation for aTS1 are presented in Fig. 1 of Supplementary material. As C1 approaches Pd, the simultaneous cleavage of the C1–I bond occurs (Table 2), and the intermediate complex aI2 is formed. aI2 exhibits a slightly distorted square planar coordination (Table 3). The NBO analysis of aI2 reveals covalent Pd–C1 and Pd–I bonds, with hybrid compositions of $0.62(sp^{0.22}d^{1.98})_{Pd} +$
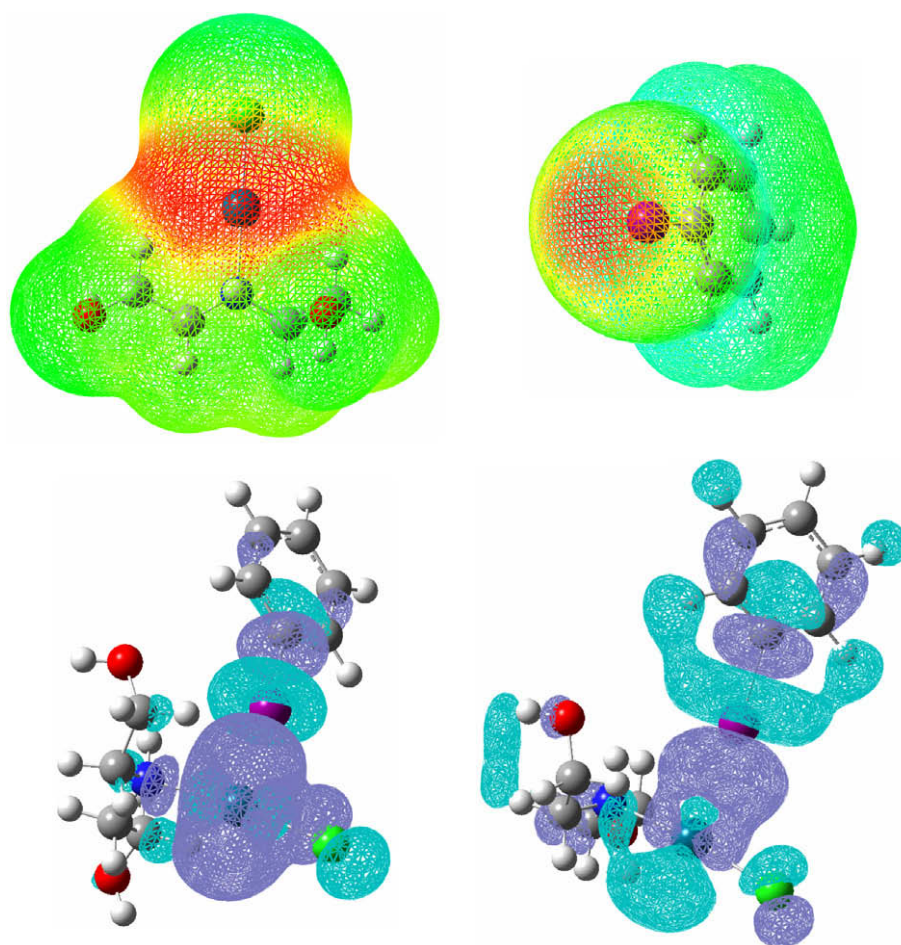
Fig. 3. HOMO map for the DEA–Pd(0)–Cl complex (top left) and LUMO map for iodobenzene (top right). HOMO (bottom left) and LUMO (bottom right) orbitals of aI1.

$0.78(sp^{3.24})_{C1}$, and $0.51(sp^{0.37}d^{0.86})_{Pd} + 0.86(sp^{5.19})_I$, respectively. A low occupancy of 1.84 in the σ Pd–C1 orbital is a consequence of its delocalization into the σ^* antibonding Pd–I orbital. Gain of occupancy in this antibonding orbital can be directly correlated with a slight weakening and elongation of the Pd–I bond, in comparison to aTS1 (Table 2). As the phenyl group and iodine are bonded to Pd, the oxidative addition is realized in pathway A. On the other hand, Pd is still coordinated with Cl and DEA (Table 2), which is confirmed with strong donation of density from the lone pairs on Cl and N ($sp^{2.58}$ and $sp^{4.77}$ orbitals whose occupancies are 1.78 and 1.73, respectively), to the formally empty $sp^{4.22}d^{0.07}$ orbital of Pd.

2.1.2. Pathway B

It is reasonable to expect that electron-rich Pd of the activated complex can attack the benzene ring and build a π complex, due to the capability of the π electron system of benzene to delocalize an excess of electrons. This assumption was confirmed with pathway B (Scheme 2), where the mechanism begins with the coordination of Pd with the C3–C4 bond. This process occurs via bTS1 (Fig. 2), and requires an activation energy of 5.2 kJ/mol. In bI1 the NBO charge of Pd (-0.043) is higher than it is in the activated complex (-0.361), whereas the NBO charges on the C atoms of the benzene ring are lower than they are in iodobenzene. For example, the NBO charges on the C3 and C4 atoms in iodobenzene amount -0.184 and -0.203, whereas the charges of the same atoms in bI1 are equal to -0.243 and -0.249. In addition, the NBO analysis of bI1 shows strong donation of density from each π bonding orbital to two adjacent π^* antibonding orbitals, confirming the delocal-

ization of electrons in the six-membered ring. There is also a strong donation of density from a d orbital of Pd (with, consequently, low occupancy of 1.63) to the π^* antibonding C3–C4 orbital. In the further course of the reaction, the investigated molecular system suffers a few rearrangements along the perimeter of the benzene ring, which enable Pd to approach I (see Pd–I distances in Table 2). In this manner intermediates bI2 and bI3 are formed via transition states bTS2 and bTS3 (Scheme 2, Fig. 2), with the activation energies of 8.0 and 17.1 kJ/mol (Table 1 of Supplementary material, Fig. 1). The crucial feature of bTS2 is that Pd is not coordinated with N (Table 2). From this stage of the reaction the DEA molecule acts as a molecule of solvent. Here we present the results of the investigation where the DEA molecule is included in the calculation, as the hydrogen of its hydroxyl group (H1 in Scheme 2 and Fig. 1) forms strong hydrogen bonding with the chlorine, and influences upon the structures and energies of transition states and intermediates. In bI2 Pd is coordinated with Cl and the C2–C3 bond, which is documented with the delocalization of the $sp^{2.41}$ orbital of Cl (whose occupancy is 1.80) into the formally empty $sp^{0.05}d^{0.08}$ orbital of Pd (whose occupancy is 0.27), and the delocalization of a d orbital of Pd (whose occupancy is 1.69) into the π^* antibonding C2–C3 orbital. In bI3 there are significantly low occupancies in a d orbital of Pd (1.64), $sp^{2.31}$ orbital of Cl (1.80), and π bonding $0.74(p)_{C1} + 0.67(p)_{C2}$ orbital (1.68). The lone pair on Pd delocalizes into the π^* antibonding C1–C2 orbital, whereas the lone pair on Cl and the π C1–C2 orbital delocalize into the formally empty $sp^{0.05}d^{0.07}$ orbital of Pd. In the further course of the reaction intermediate bI4 is formed via early transition state bTS4, requiring an energy of activation of only 0.7 kJ/mol. The main feature

of bTS4 and I4 is that Pd exhibits a distorted trigonal coordination (Table 3). Tricoordinated Pd complexes are known in literature [15,16,21–23]. In bTS4 the weak Pd–C1 bond is formed. Pd is not coordinated with C2, and the Pd–I bond is being formed. In bI4 Pd forms covalent bonds with C1 and I whose hybrid compositions are $0.68(sp^{0.11}d^{2.12})_{Pd} + 0.73(sp^{3.85})_{C1}$ and $0.47(sp^{0.32}d^{0.71})_{Pd} + 0.88(sp^{5.76}d^{0.01})_I$. Pd is also coordinated with Cl, which is documented with a delocalization of the lone pair on Cl ($sp^{4.68}$ orbital with an occupancy of 1.71) into the formally empty $sp^{4.81}d^{0.10}$ orbital of Pd.

The geometries of bI2, bTS3, bI3, bTS4, and bI4 are calculated in the absence of the DEA molecules. Their structures are presented in Fig. 1, selected bond distances and angles are given in Tables 2 and 3, whereas total energies, enthalpies, and free energies are given in Table 4 of Supplementary material. Comparison of these structures to the geometries of the analogous species in the presence of DEA undoubtedly shows strong influence of hydrogen bonds to the course of the reaction. The presence of DEA as solvent lowers the activation energies for the formation of all transition states in pathway B (Tables 1 and 4 in Supplementary material). As DEA is used as solvent in the reaction performed in the absence of a strong base, we assume that this influence is in reality even stronger.

Comparison of the structures and energies for bI2 and bI4 reveals some similarities and significant differences. The Pd–C1 and Pd–I bonds are established in both species, and there are four lone pairs in almost pure d orbitals on Pd. On the other hand, there is steric hindrance induced with the ligating DEA molecule in aI2, whereas Pd in bI4 is still low-ligated. The ΔG^{298} value for bI4 is higher than that for aI2 by 25.5 kJ/mol. These facts indicate that bI4 is more reactive and structurally more favorable for migratory insertion step (**c** in Scheme 1) than aI2. In addition, the energetics of the two pathways shows that the activation energy for the formation of aTS1 is considerably higher than those required for the formation of all transition states in pathway B. Thus, we can conclude that pathway B provides significantly more favorable mechanism for the oxidative addition of iodobenzene to the DEA–Pd(0)–Cl complex. The influence of different aryl halides and substituents on the phenyl group is under intense examination.

Our papers on the preactivation reaction of the *trans*-dichlorobis(diethanolamine-*N*)palladium(II) complex showed that this process requires noticeable higher activation energies than those required in pathways A and B. Thus, our investigations indicate that oxidative addition is not the rate determining step in the catalytic cycle presented in Scheme 1. A conviction that oxidative addition is the rate determining step can be a consequence of the fact that the activation energies for the preactivation reaction have been provided only recently [11,12].

3. Material and methods

The reactions were monitored and analyzed with GC chromatography and ^{1}H NMR spectroscopy. GLC analyzes were obtained with an Agilent 6890N (G 1530N) instrument (Serial # CN10702033), with capillary apolar column. The ^{1}H NMR spectra were run in CDCl$_3$ on a Varian Gemini 200 MHz spectrometer. For column chromatography silica gel 60 (Merck, particle size 0.063–0.200 mm) was used. The compounds PdCl$_2$, diethanolamine, aryl iodides and olefins were obtained from Aldrich Chemical Co.

3.1. General procedure for the reactions of olefines and aryl iodides catalyzed by trans-[PdCl$_2$(DEA)$_2$]

For the synthetic simplicity the catalyst *trans*-[PdCl$_2$(DEA)$_2$] was generated and preactivated in the same reaction pot where the Heck reaction of aryl iodide and appropriate olefin was performed.

To a magnetically stirred solution of 2 mol% of PdCl$_2$ (0.02 mmol) in 2 cm^3 of ethanol and 2 mol% of diethanolamine (0.02 mmol) at room temperature was added. Stirring was continued at 50–60 °C for half an hour. After the evaporation of EtOH *in vacuo*, the orange complex *trans*-[PdCl$_2$(DEA)$_2$] was obtained. The crystal structure determination of *trans*-[PdCl$_2$(DEA)$_2$], as well as selected bond distances, bond angles and hydrogen bonds, are presented in Ref. [13]. Aryl iodide (1 mmol), activated olefin (1.1 mmol) and 1.05 g DEA (1 mmol), as a solvent and weak base, were then added in the same reaction pot. The reaction mixture was stirred and heated at 110 °C for 12 h for iodobenzene, and 14 h for iodoanisole. After cooling the reaction mixture to room temperature, CH$_2$Cl$_2$ (7.0 cm^3) was added to extract the product. The organic phase was washed with water and the aqueous layer was extracted with dichloromethane (2 × 10 cm^3). The combined organic layers were dried over anhydrous sodium sulfate, and then solvent was evaporated *in vacuo*. After the extraction of the products of the first-time reaction, ethanol was added in the reaction flask (3 × 10 cm^3) to extract catalyst. After the evaporation of ethanol, the starting catalyst precursor remains. The precatalyst was reused two times without significant decrease in catalytic performance (the yields of the coupling products were to 5% lower). When the reactions were performed in the presence of strong base, equimolar ratios of aryl iodlide (1 mmol), activated olefin (1.1 mmol), 2 mol% *trans*-[PdCl$_2$(DEA)$_2$], and 0.20 mmol NaOEt were mixed. The reaction were performed at 90 °C, in CH$_3$CN as solvent (1 cm^3), in a duration of 8 h for iodobenzene and for 10 h for iodoanisole. The reaction mixtures were separated with column chromatography on silica gel (dichloromethane as solvent). The isolated known coupling products **1–8** were analyzed and characterized on the basis of their spectroscopic data, and by comparing these data to the spectra of the commercially available compounds. The ^{1}H NMR spectra of the products **1–8** are presented in Supplementary material.

3.2. Computational details

All calculations were conducted using Gaussian03 [34] with the B3LYP hybrid functional [35–37]. The triple split valence basis set 6-311G(d,p) was used for C, H, O, N, Cl, and I [38], whereas LANL2DZ + ECP [39] was employed for the Pd center. Geometrical parameters of all investigated species were optimized in vacuum. Vibrational analysis was performed for all structures. All calculated structures were verified to be local minima (all positive eigenvalues) for ground state structures, or first-order saddle points (one negative eigenvalue) for transition state structures, by frequency calculations. The natural bond orbital analysis [40] (Gaussian NBO version) was performed for all structures. According to this method, delocalization of electron density between occupied Lewis type (bonding or lone pair) orbitals and formally unoccupied (antibonding or Rydberg) non-Lewis NBOs corresponds to a stabilizing donor–acceptor interaction. The strength of this interaction can be estimated by the second order perturbation theory [41]. The Rydberg NBOs (extra-valence orbitals) have relatively small occupancies, therefore they are omitted from the above discussion.

Appendix A. Supplementary material

Supplementary data associated with this article can be found, in the online version, at doi:10.1016/j.jorganchem.2009.07.043.

Z.D. Petrović et al. / Journal of Organometallic Chemistry 694 (2009) 3852–3858

References

[1] R. Heck, Acc. Chem. Res. 12 (1979) 146.
[2] D.A. Alonso, C. Nájera, M.C. Pácheco, Org. Lett. 2 (2000) 1823.
[3] I.P. Beletskaya, A.V. Cheprakov, Chem. Rev. 100 (2000) 3009.
[4] C.S. Consorti, M.L. Zanini, S. Leal, G. Ebeling, J. Dupont, Org. Lett. 5 (2003) 983.
[5] C.M. Jin, B. Twamley, J.M. Shreeve, Organometallics 24 (2005) 3020.
[6] R. Wang, B. Twamley, J.M. Shreeve, J. Org. Chem. 71 (2006) 426.
[7] X. Cui, J. Li, Z.P. Zhang, Y. Fu, L. Liu, Q.X. Guo, J. Org. Chem. 72 (2007) 9342.
[8] J.G. De Vries, Can. J. Chem. 79 (2001) 1086.
[9] B.M. Trost, in: Atta-Ur-Rahman (Ed.), Advances in Natural Product Chemistry, Harwood Academic Publishers, Harwood, 1992, p. 194.
[10] B.M. Trost, M.L. Crawley, Chem. Rev. 103 (2003) 2921.
[11] Z.D. Petrović, S. Marković, D. Simijonović, V.P. Petrović, Monatsh. Chem. 140 (2009) 371.
[12] S. Marković, Z.D. Petrović, V.P. Petrović, Monatsh. Chem. 140 (2009) 171.
[13] Z.D. Petrović, M.I. Djuran, F.W. Heinemann, S. Rajković, S. Trifunović, Bioorg. Chem. 34 (2006) 225.
[14] H.M. Senn, T. Ziegler, Organometallics 23 (2004) 2980.
[15] M. Ahlquist, P. Fristup, D. Tanner, P.O. Norrby, Organometallics 25 (2006) 2066.
[16] M. Ahlquist, P.O. Norrby, Organometallics 26 (2007) 550.
[17] L.J. Goossen, D. Koley, H. Hermann, W. Thiel, Chem. Commun. (2004) 2141.
[18] L.J. Goossen, D. Koley, H. Hermann, W. Thiel, Organometallics 24 (2005) 2398.
[19] J.C. Green, B.J. Herbert, J.R. Lonsdale, J. Organomet. Chem. 690 (2005) 6054.
[20] X. Cui, Z. Li, Z.C. Tao, Y. Xu, J. Li, L. Liu, Q.X. Guo, Org. Lett. 8 (2006) 2467.
[21] Z. Li, Y. Fu, Q.X. Guo, L. Liu, Organometallics 27 (2008) 4043.
[22] P. Surawatanawong, Y. Fan, B.M.J. Hall, Organomet. Chem. 693 (2008) 1552.
[23] Y.L. Huang, C.M. Weng, F.E. Hong, Chem. Eur. J. 14 (2008) 4426.
[24] R.J. Deeth, A. Smith, M.J. Brown, J. Am. Chem. Soc. 126 (2004) 7144.
[25] T. Kawano, T. Shinomaru, I. Ueda, Org. Lett. 4 (2002) 2545.
[26] M.R. Eberhard, Org. Lett. 6 (2004) 2125.
[27] S.C. Consorti, F.R. Flores, J. Dupont, J. Am. Chem. Soc. 127 (2005) 6411.
[28] O. Esposito, M.P.G. Pedro, K.A. Lewis, F.S. Caddick, G.N. Cloke, P.B. Hitchcock, Organometallics 27 (2008) 6411.
[29] A. Alimardanov, L. Schmieder-van de Vondervoort, A.H.M. de Vries, J.G. de Vries, Adv. Synth. Catal. 346 (2004) 1812.
[30] M.T. Lee, M.H. Lee, H.C. Hu, Organometallics 26 (2007) 1317.
[31] A.S. Gruber, D. Pozebon, A.L. Monteiro, J. Dupont, Tetrahedron Lett. 42 (2001) 7345.
[32] C. Elia, Elyashiv-Bard, A. Sen, Organometallics 21 (2002) 4249.
[33] A.C. Albiniz, P. Espinet, Lopez-Fernndez, Organometallics 22 (2003) 4206.
[34] M.J. Frisch, W.G. Trucks, B.H. Schlegel, E.G. Scuseria, A.M. Robb, R.J. Cheeseman, G.V. Zakrzewski, A.J. Montgomery Jr., E.R. Stratmann, C.J. Burant, S. Dapprich, M.J. Millam, D.A. Daniels, N.K. Kudin, C.M. Strain, O. Farkas, J. Tomasi, V. Barone, M. Cossi, R. Cammi, B. Mennucci, C. Pomelli, C. Adamo, S. Clifford, J. Ochterski, A.G. Petersson, Y.P. Ayala, Q. Cui, K. Morokuma, D.A. Malick, D.K. Rabuck, K. Raghavachari, B.J. Foresman, J. Cioslowski, V.J. Ortiz, G.A. Baboul, B.B. Stefanov, G. Liu, A. Liashenko, P. Piskorz, I. Komaromi, R. Gomperts, L.R. Martin, J.D. Fox, T. Keith, A.M. Al-Laham, Y.C. Peng, A. Nanayakkara, M. Challacombe, P.M.W. Gill, B. Johnson, W. Chen, W.M. Wong, L.J. Andres, C. Gonzalez, M. Head-Gordon, S.E. Replogle, A.J. Pople, Gaussian 03, Revision E.01-SMP, Gaussian Inc., Pittsburgh, PA, 2003.
[35] D.A. Becke, Phys. Rev. A (1988) 3098.
[36] C. Lee, W. Yang, R.G. Parr, Phys. Rev. B (1988) 785.
[37] D.A. Becke, J. Chem. Phys. 98 (1993) 5648.
[38] R. Krishnan, J.S. Binkley, R. Seeger, J.A. Pople, J. Chem. Phys. 72 (1980) 650.
[39] J.P. Hay, R.W. Wadt, J. Chem. Phys. 82 (1985) 270.
[40] E.A. Reed, B.R. Weinstock, F. Weinhold, J. Chem. Phys. 83 (1985) 735.
[41] E.A. Reed, A.L. Curtiss, F. Weinhold, Chem. Rev. 88 (1988) 899.